

Modeling Deep Brain Stimulation Based on Current Steering Scheme

Charles T. M. Choi^{1,2}, Yen-Ting Lee³, and Yi-Lin Tsou^{1,2}

¹Department of Computer Science, National Chiao Tung University, Hsinchu 300, Taiwan

²Institute of Biomedical Engineering, National Chiao Tung University, Hsinchu 300, Taiwan

³Institute of Information Science, Academia Sinica, Taipei 115, Taiwan

The goal of this paper is to develop a quantitative understanding about the shape and the volume of tissue activated (VTA) and stimulation sites by deep brain stimulation (DBS) in deep brain area like subthalamic nucleus (STN) to improve neural stimulation. Monopolar current steering approach has been studied in cochlear implants and deep brain stimulation. In this paper, novel bipolar and tripolar current steering schemes are applied to deep brain stimulation. Finite-element models of deep brain stimulation are used to study the volume of tissue activated for monopolar, bipolar, and tripolar current steering configurations.

Index Terms—Bipolar, current steering, deep brain stimulation, finite-element method, monopolar, tripolar.

I. INTRODUCTION

DEEP BRAIN STIMULATION (DBS) is a surgical treatment involving the implantation of a medical device which consists of three components: the implanted pulse generator (IPG), the lead with four platinum iridium electrodes, and the extension. All three components are surgically implanted inside the body. It is an effective, proven therapy for the treatment of Parkinson's disease (PD), essential tremor, and dystonia. So far, high frequency DBS is known to change brain activity analogous to those achieved by surgical lesions, its effects are reversible (turn on/off the electrode can inhibit/recover activity in brain) [1].

The fundamental objective of DBS is to modulate the neural activity with extracellular electric fields, but the technology necessary to predict accurately and visualize the neural response to DBS has not been previously available.

Existing DBS system were adapted from cardiac pacing technology ~20 years old. The original design of the Medtronic 3387/3389 DBS electrode was hindered by limited knowledge of the neural stimulation objectives of the device. In this paper, we will study the volume of tissue activated (VTA) generated by using deep brain stimulation using a current steering scheme [2]. The innovation of this paper is to extend the prediction of the shape and volume of tissue activated [3]–[7] using a current steering scheme [2] from monopolar [8] to bipolar and tripolar stimulation configurations with and without an encapsulation or tissue layer. Instead of relying on trial and error, this result allows DBS clinicians to visualize the effect of DBS program parameter changes and allow them to do the “what if” analysis.

II. METHODS

A. Finite-Element Model (FEM) of Human Brain Tissue and DBS Lead Electrode

An FEM of brain tissues and DBS leads to address the effects of deep brain stimulation in an inhomogeneous medium

Manuscript received May 31, 2010; accepted August 31, 2010. Date of current version April 22, 2011. Corresponding author: C. T. M. Choi (e-mail: c.t.choi@iee.org; ctchoi@cs.nctu.edu.tw).

Color versions of one or more of the figures in this paper are available online at <http://ieeexplore.ieee.org>.

Digital Object Identifier 10.1109/TMAG.2010.2076795

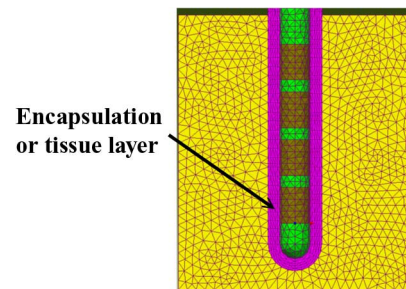


Fig. 1. Shows an FEM with about 300 000 finite-element nodes. The green part shows an electrode array; the purple part shows an encapsulation or tissue layer with a width of 0.5 mm and conductivity of 0.1 S/m, and the yellow part show the surrounding tissue (gray matter) with an isotropic conductivity of 0.2 S/m [8].

was created. In our finite element model (see Fig. 1), an axisymmetric FEM model of DBS electrodes with approximately 300 000 nodes were constructed. Electrode contact dimensions are 1.5 mm in height and 1.27 mm in diameter. These dimensions were based on the Medtronic 3387/3389 DBS electrode contact dimensions [4]. The DBS electrode carrier was modeled as an electrical insulator and the DBS electrode contact was used as a voltage source.

After the electrical potential distribution of the DBS model was computed by solving Poisson's equation, it can be used to compute the current distribution in the tissues around the DBS electrodes. First, we convert the potential distribution generated within the tissue to current distribution by

$$I_{\text{int}}(n) = G_i(-) [V(n-1) - V(n)] + G_i(+) [V(n+1) - V(n)] \quad (1)$$

where $I_{\text{int}}(n)$ represents the intra-membrane current in node n shows in Fig. 2, $V(n)$ represents the voltage of node n . $G_i(-)$ represents the inter-segmental conductance between the n and $n-1$ compartments and $G_i(+)$ represents the inter-segmental conductance between the n and $n+1$ compartments of the neuron in the FEM. VTA was computed from the DBS FEM model coupled with 5.7 μm diameter myelinated axon models. Each axon was oriented perpendicular to the lead electrode, including 21 nodes of Ranvier with 0.5 mm internodal spacing, and total neuron array size are 7×11 [5].

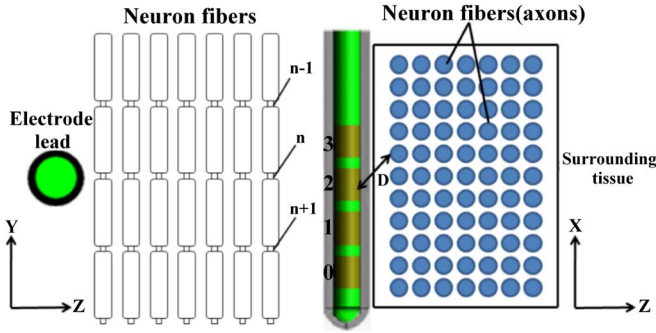


Fig. 2. (left) Shows a DBS electrode lead with neuron fibers or axons, each neuron fiber or axon has 21 nodes, e.g., node n . D represents the distance between electrode contact and axon. Each electrode contact is labeled from top to bottom as 3 to 0 (right).

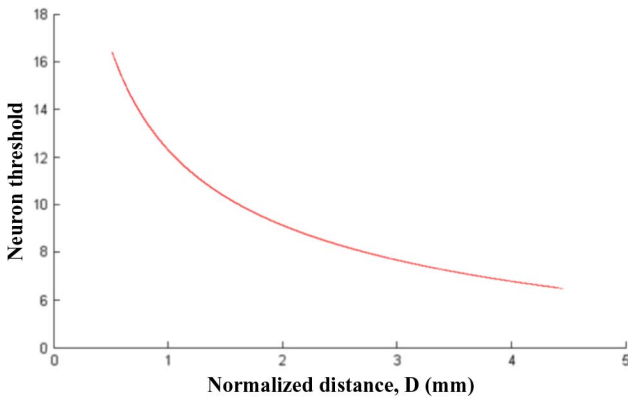


Fig. 3. Relationship between neuron threshold and normalized distance D .

Next, the current distribution can be used to compute VTA. we will show the detail of the VTA computation and the effect of changing the stimulation configuration and stimulation parameters will have on the VTA. Second, we will also address the effect of current steering on the shape of VTA.

B. Neuron Threshold Prediction

A method to predict excitation thresholds for axons using linear models and a predetermined critical voltage [6] is given. Equations (2) and (4) are used to determine the relationship between neuron threshold and normalized distance D on monopolar and bipolar configurations (see Fig. 3)

$$1/D = \text{contact } 1/\text{axon1} + \text{contact } 2/\text{axon2}. \quad (2)$$

Likewise, (3) and (4) are used to determine the relationship between neuron threshold and normalized distance on tripolar configuration (see Fig. 3) [8]. Extending (2) to tripolar configuration, normalized distance D is defined by

$$1/D = \text{contact } 1/\text{axon1} + \text{contact } 2/\text{axon2} + \text{contact } 3/\text{axon3} \quad (3)$$

$$\text{Neuron threshold} = 12.3 * D^{-0.43} \quad (4)$$

where contact 1, contact 2, and contact 3 are the voltages of electrode contact 1, 2, and 3, respectively, and axon1, axon2, and axon3 are the distance from axon to contact 1, 2, and 3, respectively (see Figs. 2, 4, and 5).

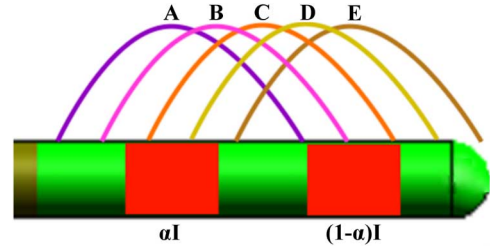


Fig. 4. For monopolar current steering scheme, a different electric current spread and stimulation site such as “A”, “B”, “C”, “D”, or “E”.

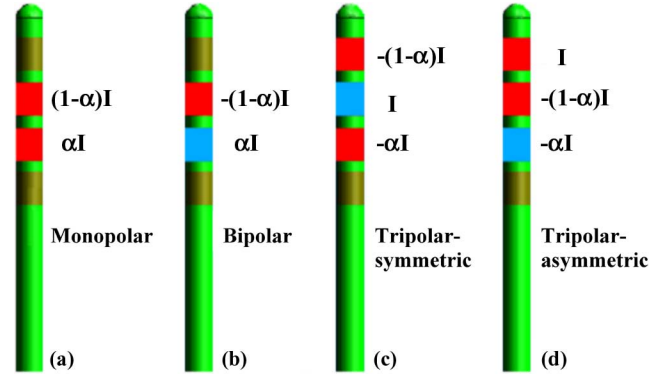


Fig. 5. Three types of current steering stimulating configurations, including monopolar, bipolar, and tripolar stimulating configurations, are shown. Tripolar is divided into symmetric and asymmetric stimulating configurations.

Finally, if the result of (1) is over the threshold as determined by Fig. 3, it is counted as a part of the VTA.

C. Current Steering Scheme

Current steering scheme has been used in cochlear implant to control the location of the stimulation sites [2]. Current steering scheme operates by controlling the current ratio between neighboring electrodes. The current delivers from the left electrode is αI and the current delivers by the right electrode is $(1-\alpha)I$ as shown in Fig. 4, where $0 < \alpha < 1$.

For instance, if α equals to 0, a current spread “E” will be generated. The stimulation site would be at “E”. As α value gets larger, the stimulation site would move away from “E” toward “A”, when $\alpha = 1$.

In this paper, we introduce three types of current steering configurations, monopolar, bipolar, and tripolar, with each configuration having its own property and distinct VTA shape.

Fig. 5 shows three types of current steering stimulation schemes, including monopolar, bipolar, and tripolar configurations. Fig. 5(a) shows the monopolar current steering stimulation scheme, which has been used extensively in cochlear implants. In this scheme, two neighboring electrodes are turned on simultaneously, i.e., in phase, while adjusting α can move the peak stimulation site (see Fig. 4). Fig. 5(b) shows the bipolar current steering stimulation scheme, which imposes 180° out of phase electric current to two neighboring electrodes. This scheme will generate a twin peaks in the VTA and has not been used in any application. Fig. 5(c) and (d) show two types of tripolar current steering schemes: symmetric and asymmetric. Unlike the monopolar and bipolar schemes, in the

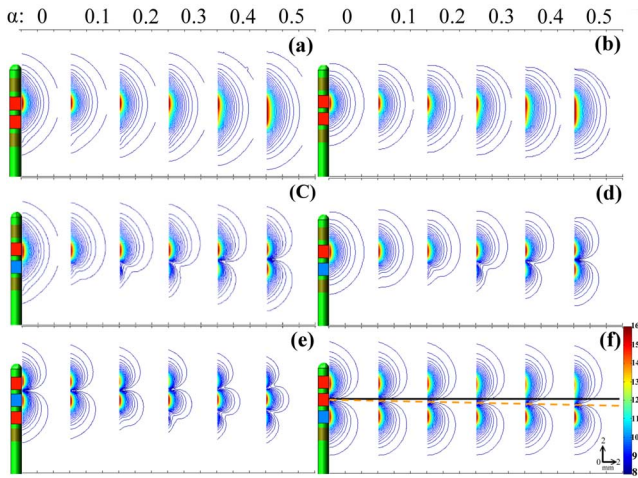


Fig. 6. (a)–(f) show the VTA for four current steering schemes. (a) and (b) show the VTA cross section for monopolar stimulation schemes without encapsulation layer and with encapsulation layer, respectively. (c) and (d) show the VTA cross section for bipolar stimulation schemes without encapsulation layer and with encapsulation layer, respectively. (e) shows the VTA cross section for tripolar-symmetric scheme with encapsulation layer. (f) shows the VTA cross section for tripolar-asymmetric scheme with encapsulation layer. All the VTA results are based on normalized input power of 0.005 W.

tripolar strategy, the sum of the electric current at any instant is zero. The total current $-\alpha I$ and $-(1-\alpha)I$ from two electrodes equals to $-I$, adding this to the current I from the third electrode will yield a net current of zero. It means electric current flow locally between the three electrodes, contrast sharply with monopolar and bipolar schemes, which direct a portion of the electric current to the ground of the system. In short, monopolar current steering configuration applies electric current that is in phase on two neighboring electrodes. Consequently, the electric current flows from electrodes to the system ground, which is usually the casing of the electric stimulator or IPG, and vice versa at a different period of the stimulation cycle. The electric current spread and the volume of tissue activated will be larger for the monopolar scheme than those from the bipolar and tripolar schemes.

III. RESULTS

All the results in this section are generated with biphasic stimulation pulse with pulse width (0.1 ms) and frequency (130 Hz) [8]. Results are divided into three parts, monopolar, bipolar, and tripolar configurations. Monopolar and bipolar configurations have two kinds of results, with and without an encapsulation layer. Encapsulation layer is used here to represent the tissues found typically in electrodes implant inside human bodies in clinical setting.

Fig. 6 shows the cross section of VTAs generated with an isotropic bulk tissue medium as shown in Figs. 1 and 2. The actual VTA is axis-symmetric respect to the DBS electrodes and should be viewed by rotating the VTA cross section around the DBS electrodes. A “ α ” is shown from 0 to 0.5 at the top of Fig. 6, indicating the VTA for each of the six cases as α varies from 0 to 0.5. By symmetry, the results for Fig. 6(a)–(e) are symmetric, thus, there is no need to show the results when α varies from

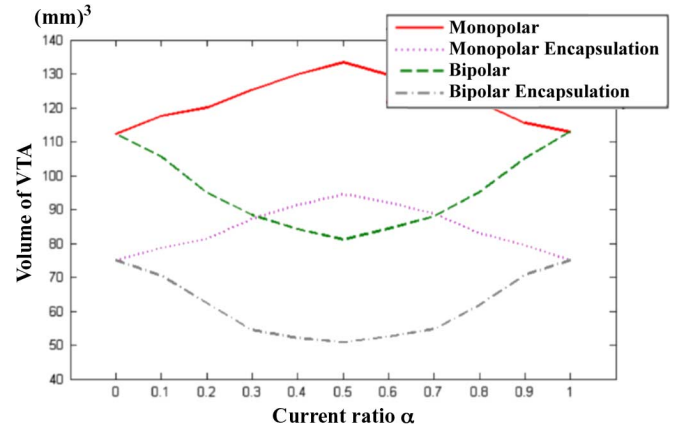


Fig. 7. Shows the relationship between the VTA and current ratio α .

0.5 to 1. All the results are based on normalized input power of 0.005 W.

By comparing the results from Fig. 6(a) and (b), the VTA contour size of the model with the encapsulation layer is smaller than those without the encapsulation layer for the monopolar current steering scheme. Likewise, the bipolar scheme shows a similar result in Fig. 6(c) and (d). The VTA contour size is a little larger on the model without the encapsulation layer. In order to save space, the results from the models without encapsulation layers for tripolar symmetric and asymmetric schemes are not shown. The cross section of VTA for monopolar scheme [see Fig. 6(a) and (b)] have one main “peak” as α varies from 0 to 0.5. Notice the centroid of the VTA moves gradually from the top electrode ($\alpha = 0$) to the space between the two electrodes ($\alpha = 0.5$), which is consistent with published result in monopolar current steering scheme [8].

The VTA cross section for the bipolar scheme [see Fig. 6(c) and (d)] moves from one main “peak” to twin “peaks” as α varies from 0 to 0.5. The centroid of the single “peak” VTA moves gradually from the top electrode ($\alpha = 0$) to the twin “peaks” centered near both electrodes ($\alpha = 0.5$).

The VTA cross section for the tripolar symmetric scheme [see Fig. 6(e)] moves from twin “peaks” to triple “peaks” as α varies from 0 to 0.5. The centroid of the twin peaks centered at the top two electrodes ($\alpha = 0$) to the triple “peaks” centered at the three electrodes ($\alpha = 0.5$). The twin “peaks” of VTA cross section for the tripolar asymmetric scheme [see Fig. 6(f)] remains unchanged as α varies from 0 to 0.5. The centroid of the twin peaks stay at the top and third electrodes ($\alpha = 0$ to 0.5). The null moves gradually as shown in the dash line in Fig. 6(f).

A. Volume of Tissues Activated (VTA)

In addition to study the number and the shape of the peaks of the VTA cross section, we study the VTA by measuring it quantitatively. Fig. 7 shows the VTA for the monopolar and bipolar current steering scheme with and without encapsulation layers as the current ratio α varies from 0 to 1. VTA for the monopolar scheme increases as α increase from 0 to 0.5 and decreases as α increase from 0.5 to 1. The results for bipolar scheme are opposite to those from the monopolar schemes. The results for the bipolar scheme show VTA decreases as α increase from 0 to 0.5

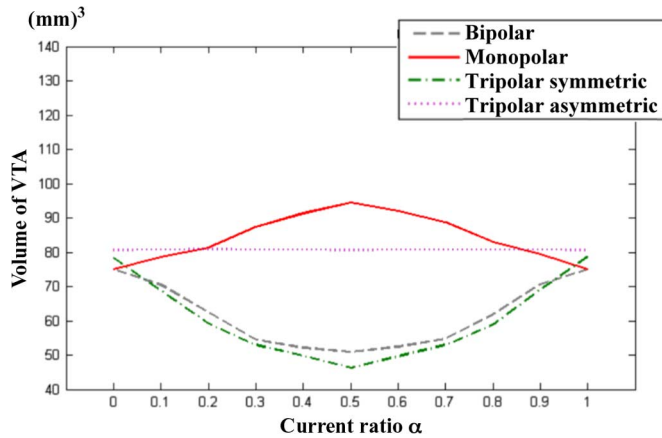


Fig. 8. Shows the relationship between the VTA and α (all with encapsulation layers or tissue layers).

and increases as α increase from 0.5 to 1. The VTA of the bipolar scheme is significantly lower than those from the monopolar scheme. VTA of monopolar, bipolar, tripolar-symmetric, and tripolar-asymmetric current steering schemes (all with encapsulation layers) are compared. One can observe that the size of VTA is the smallest and roughly the same for tripolar-symmetric and bipolar schemes. Interestingly, the size of the VTA remains unchanged as α varies from 0 to 1 for the tripolar-asymmetric scheme. Clinicians who do DBS programming can take advantage of this information to manipulate the site of the stimulation by using the monopolar current steering scheme as α varies from 0 to 1. Alternatively, they can also make use of the “peaks” in the bipolar and tripolar-symmetric current steering scheme to selectively activate certain volume of tissues surrounding the DBS electrodes. The tripolar-asymmetric scheme might be the most ineffective scheme among all four schemes because it does not alter the stimulation sites.

IV. CONCLUSION

This paper compares the size of the volume of tissue activated and number of “peaks” for monopolar, bipolar, tripolar-

symmetric, and tripolar-asymmetric current steering stimulation schemes for deep brain stimulation. Monopolar stimulation scheme offers the simplest form of stimulation control—a single “peak” can be controlled by adjusting the current ratio, α , yet the beam width is the largest among all four schemes. Tripolar-symmetric and bipolar stimulation schemes offer a more complicated control and yet generate a narrower beam width, thus, provide a more selective electrical stimulation than the monopolar scheme. The tripolar-asymmetric scheme is the most ineffective among all four schemes. The modeling results show that encapsulation layers or tissue layers would reduce the VTA. Since there is always some tissue layers surrounding the DBS electrode, the VTA result with tissue layers will reflect the clinical result more accurately. Instead of using trial and error, DBS clinicians can use this result to visualize the effect of DBS program parameter changes and allow them to do the “what if” analysis.

REFERENCES

- [1] P. Ashby, Y. J. Kim, R. Kumar, A. E. Lang, and A. M. Lozano, “Neurophysiological effects of stimulation through electrodes in the human subthalamic nucleus,” *Brain*, vol. 122, pp. 1919–1931, 1999.
- [2] C. T. M. Choi and C. H. Hsu, “Conditions for generating virtual channels in cochlear prosthesis systems,” *Annals Biomed. Eng.*, vol. 37, no. 3, pp. 614–624, Mar. 2009.
- [3] C. R. Butson and C. C. McIntyre, “Role of electrode design on the volume of tissue activated during deep brain stimulation,” *J. Neural Eng.*, vol. 3, pp. 1–8, 2006.
- [4] C. C. McIntyre, S. Mori, D. L. Sherman, N. V. Thakor, and J. L. Vitek, “Electric field and stimulating influence generated by deep brain stimulation of the subthalamic nucleus,” *Clin. Neurophysiol.*, vol. 115, pp. 589–595, 2004.
- [5] C. R. Butson, C. B. Moks, and C. C. McIntyre, “Sources and effects of electrode impedance during deep brain stimulation,” *Clin. Neurophysiol.*, vol. 117, pp. 447–454, 2006.
- [6] M. A. Moffitt, C. C. McIntyre, and W. M. Grill, “Prediction of myelinated nerve fiber stimulation thresholds: Limitations of linear models,” *IEEE Trans. Biomed. Eng.*, vol. 51, no. 2, pp. 229–236, Feb. 2004.
- [7] C. T. M. Choi and Y. T. Lee, “Modeling deep brain stimulation,” in *Proc. 13th Int. Conf. Biomed. Eng.*, Dec. 2008, pp. 619–621.
- [8] C. R. Butson and C. C. McIntyre, “Current steering to control the volume of tissue activated during deep brain stimulation,” *Brain Stimulation*, vol. 1, pp. 7–15, Jan. 2008.